RESEARCH PAPER

PCCP
www.rsc.org/pccp

The interaction of dolomite surfaces with metal impurities: a computer simulation study

Kat F. Austen,[ab] Kate Wright,[c] Ben Slater*[ab] and Julian D. Gale[c]

[a] *The Royal Institution of Great Britain, 21 Albemarle Street, London, UK. E-mail: kat@ri.ac.uk; ben@ri.ac.uk; Fax: +44 20 7629 3569; Tel: +44 20 7409 2992*
[b] *Department of Chemistry, University College London, Gower Street, London, UK*
[c] *Nanochemistry Research Institute, Department of Applied Chemistry, Curtin University of Technology, PO Box U1987, Perth, 6845WA, Australia. E-mail: kate@power.curtin.edu.au. E-mail: julian@power.curtin.edu.au; Tel: +61 8 9266 3554*

Received 21st July 2005, Accepted 20th September 2005
First published as an Advance Article on the web 17th October 2005

This study investigates the behaviour of selected, morphologically important surfaces of dolomite ($CaMg(CO_3)_2$), using computational modelling techniques. Interatomic potential methods have been used to examine impurity substitution at cationic sites in these surfaces. Environmentally prevalent cations were studied to this end, namely Ni^{2+}, Co^{2+}, Zn^{2+}, Fe^{2+}, Mn^{2+} and Cd^{2+}, all of which are also found as end-member carbonate minerals. Solid–solution substitution was investigated and showed that Cd and Mn will substitute from their end-member carbonate phase at either dolomite cation site. Mn is found to preferentially substitute at Mg sites, in agreement with experimental findings. For Ni^{2+}, Co^{2+} and Zn^{2+}, the magnitude of substitution energies is approximately equal for all surfaces, with the exception of the $(10\bar{1}4)$ surface. However, for the larger cations, a far greater disparity in substitution energies is observed. At a stepped surface, analogous substitutions were performed and it was found that substitution energies for all impurity cations were reduced, indicating that uptake is more viable during growth. The predominant surface, the $(10\bar{1}4)$, was solvated with a monolayer of water in order to investigate the influence of hydration on substitution energetics. The addition of water changes the relative preference for substitution of the different cations. Under aqueous conditions, the substitution energy is determined by three competing factors, the relative importance of which cannot be predicted without this type of computational investigation.

Introduction

Carbonate minerals have been shown to chemically interact with various solvated ions and molecules when exposed to aqueous solutions.[1–4] Dolomite and other common carbonate minerals are frequently exposed to aqueous solutions in nature that contain many environmentally damaging elements, such as zinc, cadmium and nickel.[5] Carbonate minerals are also often added to areas of high acidity, either in groundwater or in areas of acid mine drainage, where dissolution of the mineral gives rise to an increase in pH.[6] As a consequence, solubility of the pollutant metals decreases, it becomes less favourable for them to remain in solution, and precipitation will occur. Clearly, there is a chemical interaction between the aforementioned solvated species and the surface of the carbonate minerals, and it is important to understand the nature of these interactions in order to predict how minerals affect solution chemistry. Computational studies can provide valuable insights into various aspects of these complex systems by revealing the molecular scale processes that occur at the mineral–water interface. This work and further publications aim to evaluate the importance of the different factors contributing to impurity uptake at mineral–solution interfaces, with a view to developing a computationally inexpensive, transferable model for mineral–aqueous solution interfaces.

Previous computational studies of impurities in dolomite[7] concentrated on impurity substitution in the bulk and on the common $(10\bar{1}4)$ surface. The effect of non-stoichiometry on these substitutions[7] was also considered. The impurities studied were the divalent cations of Mn, Fe, Cd, Co, Zn and Ni, which are often found to be present, along with dolomite, in aquatic environments. The calculated values of substitution energy indicated a strong preference of impurity elements for Ca rather than Mg sites, both in the bulk and at the surface. The segregation energy, however, was found to be an important indicator of the preference for substitution at the different cation sites. The current study extends this work to look at dolomite's other morphologically important surfaces, using an improved description of the mineral. The influence of water upon substitution energetics has been examined and the incorporation of cations at a stepped surface has been investigated. The results are rationalised in the context of uptake of cations, either from solution or from mineral sources, on dolomite crystals.

Method

The calculations were carried out using interatomic potential methods, where functions are used to model the short- and long-range interactions of atomic or ionic species in a solid. Energy minimised structures were achieved by optimising the energy of the system with respect to the ionic co-ordinates within the latest revision of the GULP program.[8] The surfaces were modelled using 2-dimensional periodic boundary conditions (PBCs). The simulation block consists of two regions: region 1 represents the model surface and the atoms within it are allowed to relax during optimisation; region 2 simulates the effect of the bulk material on region 1 and as such all ions within this block are held fixed at their optimised positions. The surface energy, or energy per unit area required to form

DOI: 10.1039/b510454h

the surface from the bulk, is calculated as follows:

$$\gamma = \frac{U_s - U_b}{A}, \quad (1)$$

where U_s is the energy of region 1, U_b is the energy of an equal number of atoms in the bulk and A is the surface area. Surface energies will be positive, and a surface is more stable the closer the value is to zero, *i.e.*: the smaller the difference between the values of U_s and U_b.

Surfaces are usually classified using the notation of Tasker[9] as type 1, 2 or 3. Type 1 surfaces can be cleaved at any depth to produce a surface layer that is charge neutral, while for type 2, this is only true for certain cleavage depths. Type 3 surfaces cannot be cleaved in such a way as to produce a charge neutral layer and hence have a large dipole moment normal to the surface. For these surfaces, the calculated energy will be related to the magnitude of the dipole, which is in turn related to the depth of the slab. In nature, these surfaces reconstruct to eliminate any dipole by the formation of defects or the addition of OH^- groups at the surface. Within the simulation, reconstruction is performed manually by shifting a proportion of the ions at the surface to the base of the block.

In this study, we have investigated impurity substitutions on the morphologically important $(10\bar{1}4)$, $(11\bar{2}0)$, $(30\bar{3}0)$ and $(10\bar{2}1)$ surfaces, the latter of which is polar. Surface super-cells were used to avoid defect self-interaction across the periodic boundary, and to facilitate study of the effect of relative substitution site on the energy of substitution. The super-cells contained the same number of formula units for each surface, so that there were 24 cations on each surface repeat unit, enabling direct comparisons when individual substitutions were made. The most morphologically important surface is known to be the $(10\bar{1}4)$ surface, and as such it has been the focus of extra study. It is well known that real surfaces contain many defects such as steps and islands, which disrupt the perfect terrace termination in the surface plane. Consequently, steps were created on the morphologically important $(10\bar{1}4)$ surface, using a method similar to that used to reconstruct the polar $(10\bar{2}1)$ surface.

The sizes of region 1 and region 2 were converged for each of the surfaces studied, such that increasing their size had negligible effect on the surface energy. The size of region 1 was converged at 14.4 Å for the $(10\bar{1}4)$ and $(11\bar{2}0)$ surfaces and at 16.7 and 16.1 Å for the $(30\bar{3}0)$ and $(10\bar{2}1)$, regions, respectively.

Substitutions of impurity cations were made on each non-polar surface at both calcium and magnesium sites. The impurities studied were Fe^{2+}, Zn^{2+}, Co^{2+}, Cd^{2+}, Mn^{2+} and Ni^{2+}, all of which are found alongside dolomite in aqueous environments, and which form end-member carbonate minerals.

Prior to carrying out substitutions at cation sites on the stepped $(10\bar{1}4)$ surface, the energetics of the different terminations were investigated. In this paper, we focus on only the most stable termination in order to understand the differences in stability at the stepped surface and the terrace. For a full investigation of step behaviour, all the terminations should be studied. The most energetically favoured configuration has an acute carbonate termination combined with a calcium ion termination, which is discussed in more detail below.

The surface energy of a surface containing impurity cations is given by:

$$\gamma = \frac{U_s - (U_b + U_{db})}{A}, \quad (2)$$

where U_s is the enthalpy of atoms in the surface region, U_b is the enthalpy of the same number of atoms in the bulk and U_{db} is the enthalpy of the defect in the bulk.

For the substitution at the surface under vacuum, the impurity cations are considered to come from the bulk end-member carbonate. So, the reaction for the substitution of a divalent impurity cation, M2, at a Ca or Mg site, denoted by M1, on the dolomite surface is given as:

$$U_{s_{pure}} + U_{M2CO_3} \rightarrow U_{s_{def}} + U_{M1CO_3} \quad (3)$$

The enthalpy of substitution for the above reaction is found using:

$$U_{subs} = \frac{(U_{s_{def}} - U_{s_{pure}}) + n(U_{M1CO_3} - U_{M2CO_3})}{n}, \quad (4)$$

where $U_{s_{def}}$ is the total enthalpy of the system with n substitutions at the surface, and $U_{s_{pure}}$ is the total enthalpy of a pure system of the same size, U_{M1CO_3} is the enthalpy of one formula unit of calcite or magnesite, depending on which cation is replaced at the surface. U_{M2CO_3} is the enthalpy of one formula unit of the carbonate mineral that corresponds to the impurity cation. For the calculation of the enthalpy per cation of multiple substitutions at both Ca and Mg sites, eqn (4) can be modified, thus:

$$U_{subs} = \frac{(U_{s_{def}} - U_{s_{pure}}) + ((n_{Ca}U_{CaCO_3} + n_{Mg}U_{MgCO_3}) - n_{Ca+Mg}U_{M2CO_3})}{n_{Ca+Mg}}, \quad (5)$$

where n_{Ca} is the number of substitutions at the Ca site, likewise n_{Mg} is the number at the Mg site, and n_{Ca+Mg} is the total number of substitutions at the surface.

Addition of a monolayer of water to the surface was attempted for all the non-polar surfaces. A variety of initial starting configurations were used, always with the water's oxygen above each surface cation. The positions of the water's hydrogen atoms were varied so that various minimised structures were achieved. However, only for the case of the $(10\bar{1}4)$ surface was there a clear global minimum. The difficulty in achieving a global minimum for monolayer coverage on the other surfaces lies in their roughness. The $(10\bar{1}4)$ surface is the most atomically smooth of the surfaces studied. The rougher the surface, the more difficult it is to find a good starting configuration for the water molecules that will minimise readily. The energy for the surface with a monolayer is given by the difference between the enthalpy of the suface with n water molecules and the dry surface plus the same number of water molecules in the gas phase.[10] It can be calculated using the following formula:

$$\gamma_{ML} = \frac{U_{s_{hyd}} - (U_b + nU_{H_2O_{(l)}})}{A} \quad (6)$$

where $U_{H_2O_{(l)}}$ is the potential enthalpy of n water molecules forming the monolayer, which is equal to the condensation energy for that number of water molecules plus the self energy of the same number of water molecules. To remain self-consistent this value is taken from the work of de Leeuw and Parker,[11] from which the parameters for water have been taken. When calculating the energy of substitution of an impurity at the hydrated surface, the energy of formation for the aqueous species must be incorporated, thus:

$$E_{subs\_wet} = \frac{U_{s_{def}} - U_{s_{pure}} - n(\Delta_{hyd}G^\circ_{M2^{2+}_{(aq)}} + \Delta_{hyd}G^\circ_{M1^{2+}_{(aq)}})}{n} \quad (7)$$

In the formula above $M2^{2+}$ denotes the impurity cation and $M1^{2+}$ is the initial surface cation, either calcium or magnesium. The quantity $\Delta_{hyd}G^\circ$ is the Gibbs free energy of hydration of the ion, calculated from experiment.[12]

The carbonate potential and its interaction with calcium were those of Rohl *et al.*,[13] which have been used to model accurately the surface reconstruction of calcite. This potential describes the polarisability of the oxygen ions using the shell model.[14] These potentials can be modified easily for use with

Table 1 Born-Mayer potentials used in this work

Born-Mayer potential: $U_r = A\exp\left(-\frac{r}{\rho}\right)$				
		A/eV	ρ/Å^{-1}	Cutoff/Å
Ca core	C core	120 000 000	0.120 00	10.0
Mg core	C core	26 164 795.4	0.120 00	10.0
Fe core	C core	90 909 090.91	0.120 00	10.0
Cd core	C core	117 575 757.6	0.120 00	10.0
Mn core	C core	98 181 818.18	0.120 00	10.0
Ni core	C core	100 606 060.6	0.120 00	10.0
Zn core	C core	89 696 969.7	0.120 00	10.0
Co core	C core	95 757 575.76	0.120 00	10.0
Fe core	O_w shell	1550.1075	0.265 07	10.1
Cd core	O_w shell	3117.3763	0.256 30	10.1
Mn core	O_w shell	1440.6645	0.272 68	10.1
Ni core	O_w shell	1176.7798	0.266 61	10.1
Zn core	O_w shell	741.1401	0.289 10	10.1
Co core	O_w shell	788.8089	0.286 30	10.1

the other carbonate minerals through combination with the potentials of Fisler *et al.*[15] to gain the cation–carbonate oxygen potential. Cation–carbon potentials (Table 1) were determined through scaling the A parameter of the Born-Mayer potential for the Ca^{2+}–C interaction from Rohl *et al.*[13] with respect to variations in ionic radius, a method that has been employed previously with success to derive potentials for ions of varying size.[16] The exception was the Mg^{2+}–C interaction which, given its importance in the dolomite structure, was varied to optimise lattice parameters and bulk modulus of dolomite and magnesite ($MgCO_3$). It was found, however, that the A parameter of the cation–carbon potential contributes minimally to the total system and as such varying its value has little effect on the bulk and surface structures studied, because the cation–oxygen potential dominates. Water potentials were those of de Leeuw *et al.*,[17] and modified by expressing the coulomb term as a Morse potential for compatibility with the program used for calculations, GULP 3.[8] The cation–O_{water} potentials for the impurity cations were scaled from the cation–$O_{carbonate}$ potential as described in Wright *et al.*[10]

Results

In this section we describe the results of our calculation on pure and defective surfaces of dolomite. The suitability of the potential parameters described in the previous section is demonstrated by comparing the calculated cell parameters and bulk moduli of dolomite and other end-member carbonates with those obtained from experiment. The data (Table 2) show that the potentials are able to reproduce the bulk properties of dolomite, with agreement between lattice parameters being very favourable, lying within 0.7% of the experimental values. Calculated data for the other end-member carbonates are also in good agreement with experiment and thus the potentials are suitable for simulating carbonate–metal interactions.

Table 3 Surface energies for $(10\bar{1}4)$, $(11\bar{2}0)$, $(30\bar{3}0)$ and $(10\bar{2}1)$ surfaces

Surface	γ/J m^{-2}
$(10\bar{1}4)$	0.55
$(11\bar{2}0)$	0.89
$(30\bar{3}0)$	0.80
$(10\bar{2}1)_{0.3718}$	0.79

Dry surface results

In the first instance, we have calculated the structure and energetics of pure dolomite surfaces under vacuum conditions. Three non-polar surfaces were studied: the $(10\bar{1}4)$, $(11\bar{2}0)$ and $(30\bar{3}0)$ surfaces, and one polar surface, the $(10\bar{2}1)$. The optimised geometries for the non-polar surfaces are shown in Fig. 1. The relaxed surface energies of the dry surfaces are given in Table 3 and show that the most stable surface is the $(10\bar{1}4)$, followed by $(10\bar{2}1)$, $(30\bar{3}0)$ and then the $(11\bar{2}0)$ surface. This follows similar trends to those previously reported,[17] although the magnitude of the surface energies is slightly lower, and the relative stabilities of the $(10\bar{2}1)$ and the $(30\bar{3}0)$ surfaces are reversed, so that the $(10\bar{2}1)$ surface is more stable. The relaxation of the $(30\bar{3}0)$ surface involves distortion of the planar carbonate ion in order to stabilise the surface, and this out-of-plane bending is less favourable with the present potential model than is the case for previous models. In the present work the potential has been optimised to describe carbonate ion both in the bulk and in under-coordinated environments such as surfaces. As a consequence of this improved description, which keeps the carbonate ion more rigid with respect to torsion than previous potentials, the $(30\bar{3}0)$ surface, in which this distortion of planarity is of greater importance than at the $(10\bar{2}1)$ surface, will be less stable in comparison.

In the case of the polar $(10\bar{2}1)$ surface, 4 possible different cleavage planes were found. These result in 4 different terminations (Fig. 2): the calcium terminated surface (0.000), the carbonate-over-magnesium terminated surface (0.1218), the magnesium terminated (0.3718) and carbonate-over-calcium terminated (0.6282). All of these terminations are polar and

Table 2 (a) Bulk properties of dolomite. (b) Structural and elastic properties for the end-member carbonates from both theoretical calculations and experiment

	Literature	This work
Total lattice energy/eV	−88.32[a]	−88.29
Bulk modulus/GPa	91[b], 94[c]	93.26
a,b/Å	4.81[d]	4.80
c/Å	16.01[d]	15.89
c/a	3.33	3.31

End-member	Bulk modulus/GPa Experiment	Bulk modulus/GPa This work	a,c/Å Literature	a,c/Å This work	c/a Literature	c/a This work
$CdCO_3$	100	97	4.90, 16.39	4.88, 16.41	3.34	3.36
$CoCO_3$	124	123	4.67, 14.89	4.64, 14.88	3.18	3.20
$FeCO_3$	117	120	4.73, 15.25	4.70, 15.25	3.22	3.24
$MnCO_3$	108	107	4.78, 15.56	4.76, 15.57	3.26	3.27
$NiCO_3$	131	137	4.64, 14.73	4.61, 14.72	3.17	3.19
$ZnCO_3$	123	122	4.67, 14.88	4.64, 14.88	3.19	3.21

[a] Ref. 27. [b] Ref. 28. [c] Ref. 16 - computational study, and references therein. [d] Ref. 29. [e] Ref. 16 and references therein.

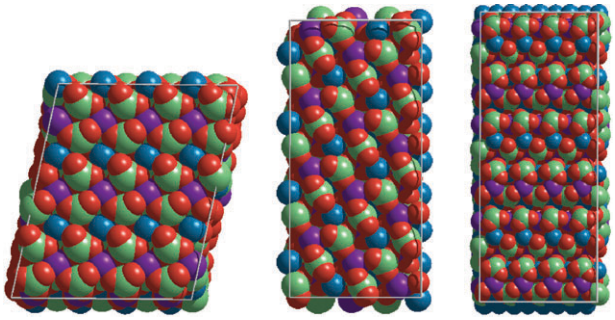

Fig. 1 Surfaces viewed from above, (left to right) $(10\bar{1}4)$, $(11\bar{2}0)$ and $(30\bar{3}0)$ [red = oxygen, green = carbon, purple = magnesium, blue = calcium].

must be reconstructed prior to relaxation. There are three possible ways of reconstructing the surface, moving surface ions either in a line parallel to the repeat unit boundaries, denoted A, in a diagonal across the cell, B, or in a triangle, C (within the 2 × 1 repeat unit). The combinations of these different surface terminations and reconstructions were investigated, and the one that yielded the lowest surface energy was selected, being the 0.3718 shift combined with reconstruction A, which was 0.13 eV more stable than the other reconstructions. Due to constraints of computational expense, only this termination and reconstruction were used to study impurity substitutions at the $(10\bar{2}1)$ surface.

On comparing the energy difference between the pure and defective surface blocks, a trend is apparent (Table 4). The calculations containing impurities at surface calcium sites were found to be consistently lower in energy than the respective pure surface cell, in accordance with earlier work on the $(10\bar{1}4)$ surface.[7] In addition, the degree of cell stabilisation varies with the ionic radius of the different cations studied, thus: $Ni^{2+} > Co^{2+} > Zn^{2+} > Fe^{2+} > Mn^{2+} > Cd^{2+}$, adhering to an inverse relationship between cationic radius and a lowering in energy of the surface. It was found that this stabilisation was evident whenever the ionic radius of the impurity cation was smaller than the substituted cation. Hence there is a stabilisation for substitutions at Mg sites for Ni, Co and Zn, because they have similar ionic radii relative to the Mg cation. All the impurity ions have smaller radii than the divalent Ca cation. Fig. 3 shows the substitution energies for the surfaces studied, calculated according to eqn (4). As shown, the dependency on the ionic radii disappears when considering the exchange of cations in a solid solution, except for substitutions at the calcium site on the $(10\bar{1}4)$ surface, which are unfavourable.

It is evident, from examination of Fig. 3, that Cd and Mn substitutions are most favourable at Mg sites on the $(11\bar{2}0)$ surface, and that these ions will also favourably substitute at the Ca site on this surface. Additionally, Zn has a very slightly negative substitution enthalpy for this surface at the calcium site. The substitution of zinc at magnesium sites is also very slightly favourable for the $(30\bar{3}0)$ and $(10\bar{1}4)$ surfaces. The preference for Mn to substitute at Mg sites in dolomite, but also to substitute at Ca sites, has been observed experimentally,[18] supporting the findings in this study. The $(10\bar{2}1)$ surface is not predicted to interact with the impurities according to the

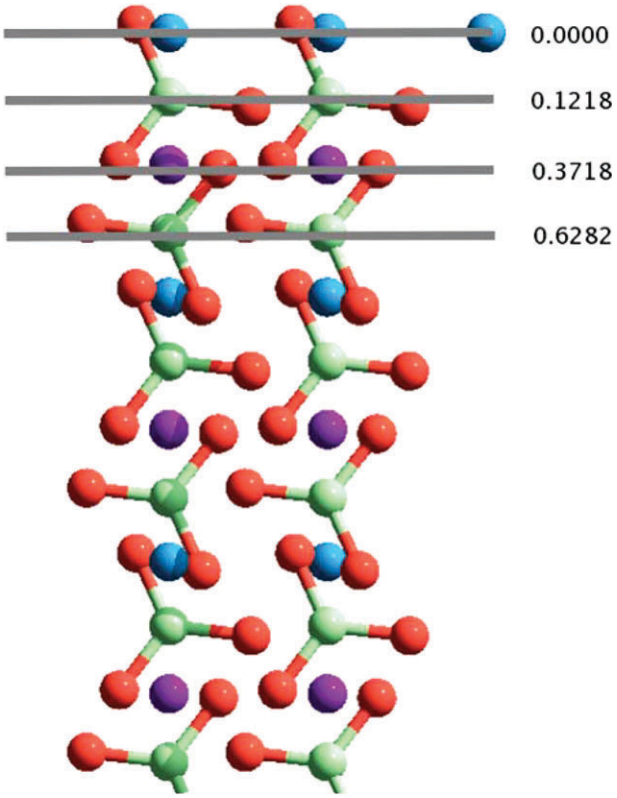

Fig. 2 Possible cuts on the $(10\bar{2}1)$ surface.

model used. The values shown for this surface are for substitutions at the most favourable site, as the surface Mg sites are inequivalent due to the reconstruction. The structure of the surface is illustrated in Fig. 4, showing that the magnesium ions sink into the surface on relaxation, resulting in significant stabilisation of the surface, reflected in the 2 eV difference in surface energies between the relaxed and unrelaxed structures. There is a slight preference for substitutions at site 1 over the other two sites. Analysis of the surface geometries shows that this magnesium cation is the least tightly bound of the three, with the largest Mg–O distances for its nearest carbonate ion.

The trend in substitution energy for each surface can be explained by the surface geometries; the distance between the cation and the atoms in its immediate vicinity (Table 5), and the differences between pure surfaces and those containing impurities. The $(11\bar{2}0)$ surface is substituted most favourably by Co, Zn, Mn and Cd cations. The structure of the $(11\bar{2}0)$ surface is the most open, the carbonate ions do not distort over or around a surface cation due to the surface structure. As can be seen from Table 5, the $(11\bar{2}0)$ surface is the most open, especially with respect to the magnesium sites. This has the most importance for the larger cations and is an explanation for the more negative substitution energies for this surface. The $(30\bar{3}0)$ surface undergoes changes in the orientation of alternate surface carbonate ions near the impurity cations introduced at calcium sites, which leads to a lowering of the surface energy. The extent of this re-orientation is far less at

Table 4 Enthalpy difference between the pure surface and the defective surface, in eV

Impurity	Ca $(11\bar{2}0)$	Ca $(10\bar{1}4)$	Ca $(30\bar{3}0)$	Mg $(11\bar{2}0)$	Mg $(10\bar{1}4)$	Mg $(30\bar{3}0)$
Ni	−3.59	−3.11	−3.52	−0.57	−0.65	−0.59
Co	−3.07	−2.61	−3.00	−0.08	−0.10	−0.08
Zn	−3.04	−2.59	−2.98	−0.06	−0.07	−0.06
Fe	−2.71	−2.32	−2.56	0.22	0.32	0.42
Mn	−2.14	−1.80	−1.96	0.73	0.93	1.03
Cd	−1.28	−1.05	−1.08	1.47	1.92	1.97

magnesium sites, where substitutions at the more open $(10\bar{1}4)$ surface are preferable to those at the $(30\bar{3}0)$ surface for the larger cations. When multiple substitutions were made at each surface, it was found that there was no marked preference for substitution site for impurity cations relative to each other.

Stepped surfaces substitutions

Steps were made on the $(10\bar{1}4)$ surface by creating a 2×2 supercell and displacing 3 Mg ions from the surface to the bottom of the simulation block. The most favourable step termination was found to be an acute termination for the carbonate ion at one edge and calcium ions at the opposite edge (Fig. 5), which was 0.02 J m^{-2} more stable than the corresponding obtuse terminated structure. This acute terminated configuration was used for the rest of the study into the behaviour of defective surfaces. This finding is in contrast to a recent study using the rigid ion model,[19] which found that for calcite the obtuse termination was very slightly (0.04 eV) more favourable than the acute termination. The rigid ion model does not fully describe the polarisability of the carbonate ion, and therefore its behaviour in such an under-coordinated environment as a step edge may not be adequately represented. As the difference in energy between the two surfaces is expected to be small, the inclusion of polarisability could reasonably be expected to affect the relative energetics of the terminations in such a way as that observed.

As with the perfect $(10\bar{1}4)$ surface, substitutions at the step edges and terrace follow the same pattern with respect to ionic radius when comparing the energies of the surface units. There was, however, a degree of directionality in the substitutions with respect to the favourability of the substitution site. Substitutions on this stepped surface are more exothermic than those on the perfect surface, showing that naturally occurring defects at the surface increase reactivity and cation exchange. Addition of charge neutral units to the step edges was also carried out and it was found, in accordance with previous findings[17,20] that the addition of one unit to form a kink is slightly energetically unfavourable, but addition of units to complete the step causes a re-stabilization of the surface.

For calcium site substitutions, it was most favourable to substitute impurity cations at the step edge. Those sites at the other end of the terrace are next favourable, and the least favourable are those in the centre of the terrace. When multiple substitutions are made, the step edge sites are substituted first, followed by one of the sites furthest from the edge. Should a substitution be made at an 'a' site in column I (Fig. 6), it is slightly more favourable, by 0.05 eV, to substitute at a 'c' site, rather than at the 'a' site in column II. Thereafter, there is little directionality apparent except that the formation of rows, and substitutions at the middle sites, are both less favourable, the appearance of the former more so.

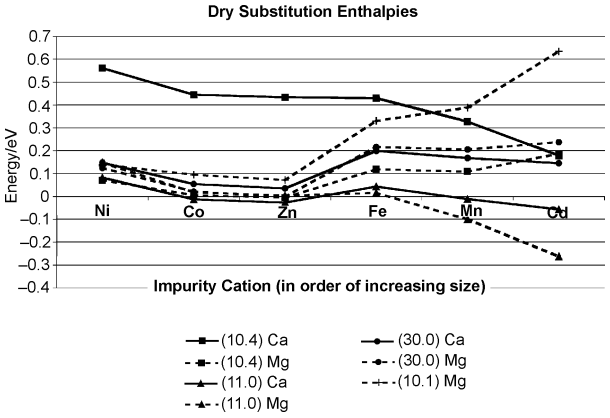

Fig. 3 Substitution energies for dry dolomite surfaces.

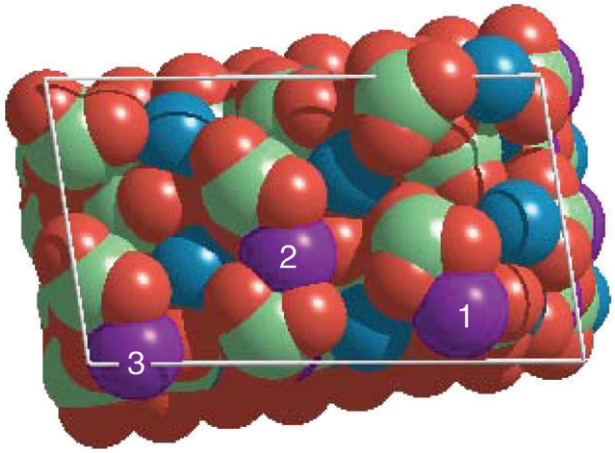

Fig. 4 View of the relaxed reconstructed $(10\bar{2}1)$ surface from above.

Fig. 7 shows that Fe impurities at the Ca site are markedly less favourable than for the other cations, although Cd is also less favourable. Examination of the surface shows that the step-site calcium ions sink into the step and surface, such that the larger cations Fe, Mn and Cd might be sterically disadvantaged for substitutions at these sites. This steric hindrance counteracts the enthalpically favoured segregation of the larger ions from their end-member carbonate minerals.

There is little difference between the substitution energies for the various cations at the Mg sites. Magnesium sites nearest the carbonate ion terminated step-edge are least favourable for substitution of any cation. It can be seen that there is reorientation of the carbonate ion at the step edge, a phenomenon seen in calcite at step edges with acute carbonate terminations.[21] This reorientation results in a reduction of 1 Å in the distance between carbonate oxygen atoms in neighbouring rows, which traps the magnesium ions in their sites. Other than the aforementioned, no significant selectivity has been observed. Multiple substitutions of the larger ions at combinations of Mg and Ca sites show that it is very slightly less favourable, by 0.06 eV, to substitute nearest neighbour sites in columns, all other things being equal. From examination of the relaxed structures it is evident that this is probably due to an increase in unfavourable steric interactions of the larger cations with the carbonate ion that they each flank.

Wet surface

In order to study the effect of hydrating the surface, water was approximated by the addition of a monolayer of water to the $(10\bar{1}4)$ surface, which is the simplest and least computationally expensive approximation. The most stable configuration formed 'bands' at the surface (Fig. 8), *via* a network of hydrogen bonds between both the water and the carbonate oxygen atoms with hydrogen atoms. Previous studies have found the most stable configuration to be one where the water molecules point in the opposite direction to that in which the carbonate ions lean.[10,17] This study, however, finds that it is energetically favourable, by 0.3 eV, for the water molecules to

Table 5 Average cation–nearest neighbour distance

Surface	Average Ca–neighbour distance/Å	Average Mg–neighbour distance/Å
$(10\bar{1}4)$	2.39	2.07
$(30\bar{3}0)$	2.35	2.01
$(11\bar{2}0)$	2.41	2.16

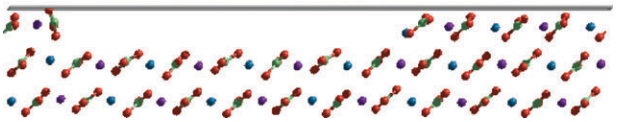

Fig. 5 Structure of the steps on the (10$\bar{1}$4) surface.

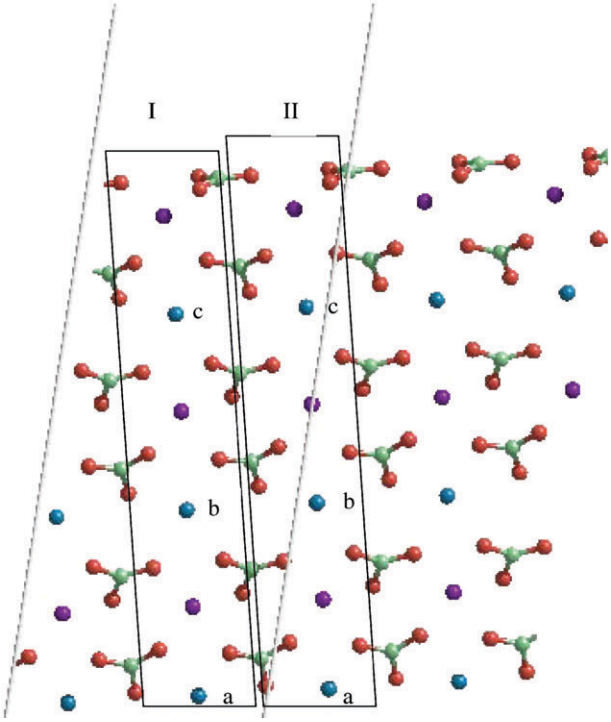

Fig. 6 Stepped surface from above.

face in the opposite direction to that previously found (Fig. 8) and form hydrogen bonds with the oxygen atoms on the carbonate ions that lean over the cation to which the water's oxygen atoms are attracted. There is also hydrogen bonding evident between the water molecules over different cations, such that the water oxygen over Mg hydrogen bonds to a hydrogen of the water above Ca, so that the water forms 'bands' along the surface in the same direction as the rows of cations. It is likely that the orientation of the water molecules and the consequent network of hydrogen bonding do not have a major influence on the energetics of substitution, as the completion of the coordination of the cations will be the factor with the strongest influence.

Upon hydration the surface is stabilised by 0.33 J m^{-2} giving a surface energy of 0.22 J m^{-2}. The cations and anions at the dry surface are under-coordinated with respect to their bulk environment, having a coordination number of 5 rather than of

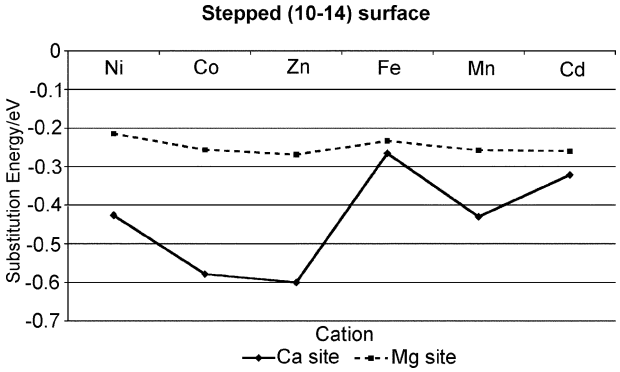

Fig. 7 Most favourable substitution energies for the (10$\bar{1}$4) surface with steps.

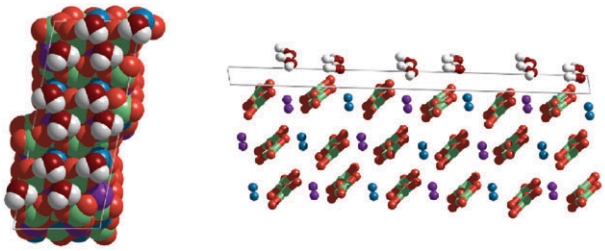

Fig. 8 Monolayer of water on the (10$\bar{1}$4) surface of dolomite: Left—from above, right—from the side showing three surface layers. Key: Ca = blue, Mg = purple, O = dark red (water)/red (carbonate), C = green.

6, respectively. The addition of a monolayer of water results in the 6th, vacant site for each cation being occupied by the water molecule's oxygen atom, so that the surface geometry is expected to more closely correspond to the bulk terminated structure, resulting in stabilization of the surface.

Substitutions were carried out on the solvated surface in the same manner as on the dry surface. Additionally, Ca and Mg impurities were included, as these cations will be present in the natural aqueous environment due to dolomite dissolution and will be in competition with the other divalent cations.[22] The substitution energies, calculated according to eqn (7), are reported in Table 6. As shown, all the energies are positive, except for the substitution of a Ca cation at a magnesium site. The preference for this substitution could be the route to magnesian calcite formation and non-stoichiometry in dolomite samples. All energies exhibit the expected behaviour of substitutions being consistently more favourable at the Mg site, which is a result of the more exothermic solvation energy of magnesium in comparison to calcium, −19.0 eV compared to −15.6 eV. This overwhelms the steric preference for calcium site substitution that is particularly important in the case of the larger cations. The self-energy of the water layer was found to be constant, regardless of the impurity substitutions. The substitution energies were found to arise from the interplay between three factors: (a) the difference in solvation energies of the cations; (b) the difference in the binding energy of the monolayer of water to the surfaces; and (c) the energetic cost of substituting an impurity at the mineral surface. The relative individual contributions of these three factors to the overall substitution energy in this aqueous model cannot be predicted *a priori* without the use of methods such as those employed in the present study.

The monolayer model does, however, have its deficiencies when used to approximate bulk water. It has been shown that at least three layers of water should be included in order to describe properly the structure of water at mineral surfaces.[23,24] Additionally, it is difficult to achieve a minimum for monolayers on rough surfaces, and the use of the current potential model does not allow for the investigation of water dissociation on the surface. It is therefore evident that a better description of solvation is necessary if substitution of aqueous species is to be calculated reliably.

Table 6 Substitution energies for (10$\bar{1}$4) surface with a monolayer of water

Cation	E_{subs} Ca site/eV	E_{subs} Mg site/eV
Cd	1.48	1.06
Co	1.57	0.66
Fe	1.26	0.47
Ni	1.75	0.75
Mn	0.79	0.09
Zn	2.06	1.11
Ca	n/a	−0.27
Mg	0.96	n/a

The results for substitutions modelled in an aqueous environment show that the dry surface substitutions do not contain sufficient information to give qualitative results on the relative cation order of substitution. It is, therefore, important to include a water model when investigating substitutions at steps. The monolayer model is inapplicable for the reasons mentioned previously, the stepped surface is too rough and will allow for too many configurations for a minimum to be reached. However, there are other problems with using the monolayer method to solvate a stepped surface. Cations at steps have more steric freedom to approach their solvated species coordination number, which is often larger than the octahedral coordination afforded by the bulk and surface-monolayer models. The perturbations in the water layer resulting from the step mean that solvation with a monolayer is even more approximate for stepped surfaces than for terraces.

Conclusions

The aim of this study is to work towards building a predictive approach capable of forecasting the uptake of metallic species onto minerals. To this end, the morphologically important surfaces of dolomite have been studied using an extended potential model to model both dry and wet terraces, and dry stepped surfaces. Substitutions of pertinent divalent cations were made at these surfaces. In the case of the dry surfaces, the substitution energy was ascertained for the interaction between dolomite and end-member carbonates, as would occur in solid-solutions. In the investigation of substitutions at wet surfaces, which was solvated with a monolayer of water, the experimental solvation energy was used to model the thermodynamic penalty of desolvating the impurity. Experimental data concerning the uptake of metal species on carbonates are mainly focused on calcite. However, site competitive behaviour is expected for dolomite because of the two distinct cation surface species which will lead to more complex substitution mechanisms. Currently, despite the importance of carbonate–aqueous interfaces, there is rather a dearth of experimental data against which predictions can be calibrated and referenced. This absence of experimental data highlights the need to develop computational models as a predictive tool, particularly as experimental means of investigating mineral–water interfacial chemical reactions pose difficulties due to reaction timescales.

The majority of relevant studies in the literature focus upon the interaction of Mn with dolomite. Thermoluminescence[25] and EPR[18] experiments have shown preferential occupation of the Mg site by Mn in geological dolomite samples, which is in agreement with the predicted site selectivity under both dry and wet conditions. For larger cations, increased selectivity of substitution is found between different growth surfaces, a phenomenon which has been observed at steps on calcite by Reeder *et al.*[26] Simulations at step sites on the $(10\bar{1}4)$ surface, showed that all substitutions were more favourable at steps than on a terrace, and this is supported by experimental studies.[26] Substitutions were universally more favourable at Ca sites than Mg sites at the obtuse step, however this may be an artefact of the geometry, so that further investigation is required to determine the selectivity definitively. In order to improve the model, alternative step geometries should be studied and, in the light of the hydrated surface results, all steps should be considered, with the use of a more sophisticated solvation model to allow for the expansion of the cation's coordination number at the step.

On analysis of the wet $(10\bar{1}4)$ surface, it was found that the substitution energy is influenced by three competing factors; the solvation energy of the interested cations, the surface–water binding energy and the exchange energy of impurities in the surface block. These solvated calculations show that the relative ordering of cation substitution in an aqueous system differs to that predicted by dry substitution calculations alone, and therefore some solvation method should be used to incorporate hydration within the model. To improve the simulation approach, a more sophisticated surface solvation model than a monolayer is necessary, in order both to fully understand the interaction of dolomite with aqueous species, and to solvate the stepped surfaces realistically. A further improvement would involve studying the barriers to inner- and outer-sphere complexation for each of the cations on dolomite, using the potential of mean force method, as recently shown by Kerisit and Parker.[23] Current work is exploiting the continuum solvation model as a computationally inexpensive method of hydrating the surface, which will be the focus of a subsequent publication. This work demonstrates the usefulness of simulation approaches in understanding the phenomenon of speciation of metal ions on mineral surfaces, and emphasises both the need to develop modelling schemes and the requirement for complementary experimental studies.

Acknowledgements

KAF would like to thank NERC for a studentship. JDG would like to thank the Government of Western Australia for support through a Premiers Research Fellowship.

References

1 A. Martin-Garin, P. Van Cappellen and L. Charlet, *Geochim. Cosmochim. Acta*, 2003, **67**, 2763–2774.
2 V. N. Makarov, S. I. Mazukhina, D. V. Makarov, T. N. Vasil'eva and I. P. Kremenetskaya, *Russ. J. Inorg. Chem. (Transl. of Zh. Neorg. Khim.)*, 2001, **46**, 1646–1654.
3 M. C. Z. Moturi, M. Rawat and V. Subramanian, *Environ. Monit. Assess.*, 2004, **95**, 183–199.
4 A. Garcia-Sanchez and E. Alvarez-Ayuso, *Miner. Eng.*, 2002, **15**, 539–547.
5 R. V. De la Villa, M. De la Flor and V. Cala, *Agrochimica*, 1997, **41**, 270–278.
6 A. Hindar, R. F. Wright, P. Nilsen, T. Laessen and R. Hogberget, *Forest Ecol. Manage.*, 2003, **180**, 509–525.
7 K. Wright, R. T. Cygan and B. Slater, *Geochim. Cosmochim. Acta*, 2002, **66**, 2541–2546.
8 J. D. Gale and A. L. Rohl, *Mol. Simul.*, 2003, **29**, 291–341.
9 P. W. Tasker, *J. Phys. C*, 1979, **12**, 4977–4984.
10 K. Wright, R. T. Cygan and B. Slater, *Phys. Chem. Chem. Phys.*, 2001, **3**, 839–844.
11 N. H. de Leeuw and S. C. Parker, *Phys. Rev. B*, 1998, **58**, 13901–13908.
12 Y. Marcus, *J. Chem. Soc., Faraday Trans.*, 1991, **87**, 2995–2999.
13 A. L. Rohl, K. Wright and J. D. Gale, *Am. Mineral.*, 2003, **88**, 921–925.
14 B. G. Dick and A. W. Overhauser, *Phys. Rev.*, 1958, **112**, 90–103.
15 D. K. Fisler, J. D. Gale and R. T. Cygan, *Am. Mineral.*, 2000, **85**, 217–224.
16 S. M. Woodley, P. D. Battle, J. D. Gale and C. R. A. Catlow, *Chem. Mater.*, 2003, **15**, 1669–1675.
17 N. H. de Leeuw, *Am. Mineral.*, 2002, **87**, 679–689.
18 J. Granwehr, P. G. Weidler and A. U. Gehring, *Geochim. Cosmochim. Acta*, 2004, **68**, A107–A107.
19 O. W. Duckworth and S. T. Martin, *Am. Mineral.*, 2004, **89**, 554–563.
20 N. H. de Leeuw, *J. Phys. Chem. B*, 2002, **106**, 5241–5249.
21 N. H. de Leeuw and T. G. Cooper, *Cryst. Growth Des.*, 2004, **4**, 123–133.
22 T. Stafilov, D. Zendelovska, G. Pavlovska and K. Cundeva, *Spectrochim. Acta, Part B*, 2002, **57**, 907–917.
23 S. Kerisit and S. C. Parker, *Chem. Commun.*, 2004, 52–53.
24 C. Zhang and P. J. D. Lindan, *J. Chem. Phys.*, 2003, **119**, 9183–9190.
25 T. Calderon, P. D. Townsend, P. Beneitez, J. Garcia-Guinea, A. Millan, H. M. Rendell, A. Tookey, M. Urbina and R. A. Wood, *Radiat. Meas.*, 1996, **26**, 719–731.
26 R. J. Reeder, *Geochim. Cosmochim. Acta*, 1996, **60**, 1543–1552.
27 N. L. Ross and R. J. Reeder, *Am. Mineral.*, 1992, **77**, 412–421.
28 J. Z. Zhang and R. J. Reeder, *Am. Mineral.*, 1999, **84**, 861–870.
29 I. Martinez, J. Z. Zhang and R. J. Reeder, *Am. Mineral.*, 1996, **81**, 611–624.

